

## An ancient olive tree in the garden. Mapping the deep history of land use from a single image

Vincenza Ferrara & Anders Wästfelt

To cite this article: Vincenza Ferrara & Anders Wästfelt (2025) An ancient olive tree in the garden. Mapping the deep history of land use from a single image, Geocarto International, 40:1, 2471090, DOI: [10.1080/10106049.2025.2471090](https://doi.org/10.1080/10106049.2025.2471090)

To link to this article: <https://doi.org/10.1080/10106049.2025.2471090>



© 2025 The Author(s). Published by Informa UK Limited, trading as Taylor & Francis Group



[View supplementary material](#)



Published online: 03 Mar 2025.



[Submit your article to this journal](#)



Article views: 125



[View related articles](#)



[View Crossmark data](#)



# An ancient olive tree in the garden. Mapping the deep history of land use from a single image

Vincenza Ferrara<sup>a,b</sup> and Anders Wästfelt<sup>b</sup>

<sup>a</sup>Department of Archaeology and Ancient History, Uppsala University, Uppsala, Sweden;

<sup>b</sup>Department of Human Geography, Stockholm University, Stockholm, Sweden

## ABSTRACT

Landscapes with a deep history of land use are the legacy of millennial interactions between ecological, social and cultural elements, which can be investigated to obtain new knowledge about our present-day ecosystems. This paper presents the application of a supervised contextual post-classification technique to extract, from a single orthoimage, geospatial objects (classes) representing different temporalities of the same land use in a historical landscape. With a rural area of Sicily as case study and its century-old olive trees as geospatial 'control points', we analyse the degree of category similarity between historically contingent classes of the same land use. We map and interpret from present space their dynamics of change and persistence over time, cross-validating our results with evidence from local plant microfossils (phytoliths) analysis. We demonstrate how Earth observation products and contextual geospatial analysis are multidimensional sources of information enriching our understanding of past-present landscapes and their biocultural heritage.

## ARTICLE HISTORY

Received 20 September 2024

Accepted 18 February 2025


## KEYWORDS

Conceptual spaces; land use; context; semantic similarity

## 1. Introduction

The root and solutions to emerging environmental problems worldwide (e.g. biodiversity loss, global warming, soil degradation) rely on our capacity to better understand ecological, social and cultural processes spanning over the long term, as they shape our present-day ecosystems (Crumley 2019; de Bremond 2021; Gillson et al. 2021). Current landscapes and their land uses depend on previous land uses and, consequently, present land use will affect future practices and ecosystems (Barthel et al. 2013; Cevasco et al. 2015; Cohen et al. 2023). As such, landscapes with a deep history of a certain land use can be investigated as 'long-term experiments in agriculture' to understand the significance of certain cultivation practices on the local environment from past to present. The possibility of such investigation relies on the existence and persistence of certain biophysical elements in such historical landscapes, as being the legacy of millennial interactions

**CONTACT** Vincenza Ferrara  [vincenza.ferrara@arkeologi.uu.se](mailto:vincenza.ferrara@arkeologi.uu.se)

 Supplemental data for this article can be accessed online at <https://doi.org/10.1080/10106049.2025.2471090>.

© 2025 The Author(s). Published by Informa UK Limited, trading as Taylor & Francis Group

This is an Open Access article distributed under the terms of the Creative Commons Attribution License (<http://creativecommons.org/licenses/by/4.0/>), which permits unrestricted use, distribution, and reproduction in any medium, provided the original work is properly cited. The terms on which this article has been published allow the posting of the Accepted Manuscript in a repository by the author(s) or with their consent.

between ecological and cultural elements. These ecocultural legacies constitute the biocultural heritage of historical landscapes (Ferrara et al. 2022). A key example of landscapes with a deep history of land use persistence is represented by Mediterranean historical olive agroecosystems (Ferrara 2024). These are current agroecosystems characterised by the presence of remnants of century-old olive trees (*Olea europaea* L.) (Figure 1), as in the island of Sicily and in the case study presented in this paper. As such, they are *historical* agroecosystems since the cultivation of the olive and the olive trees themselves have been maintained for centuries, even millennia, being now a biocultural heritage as the ongoing result of different ecological, broader environmental and socio-cultural processes happening at multiple spatial and temporal scales.

These historical landscapes that we see in the present moment are thus a *juxtaposition* (cf. Hägerstrand 1991, 51) of a mixed assortment of entities, emerging as the accumulation of results from past processes through space-time (cf. Massey 1999). What we observe today is just a *spatial cross-section of time* (cf. Hägerstrand 1991, 54) of the progressive heterogeneous accumulation of legacies from past states.

From the perspective of land use classification, it is common to distinguish distinct land cover patches corresponding to diverse land use purposes, within a heterogeneous mosaic of agroecosystem types (e.g. orchards, arable fields, vineyards, gardens, and forest). In Figure 2, it is shown an olive landscape in Sicily, which is classified as one land use and land cover class, ‘olive groves’, by CORINE Land Cover (CLC) (European Environmental Agency [EEA] 2020). Nevertheless, within this class ‘olive groves’, we can *also* identify a multitude of different local spatial configurations of the same land use, featured by the peculiar ways olive trees are spatially arranged: olive trees randomly placed and at wide distances among each other, or intercropped with other trees, single olive trees within empty fields or in arable fields, or young olive trees planted in straight lines. In other words, these diverse spatial configurations of olive trees represent how people arranged the local space for agricultural purposes, maintaining the same land use (olive cultivation) but changing practices over time and consequent related spatial configurations of vegetation elements in the fields.

Although these diverse spatial configurations can be generalised as the CLC class ‘olive groves’, each of them has been created by locals in different temporal and environmental circumstances, socio-cultural contexts, for diverse purposes and responding to both individual and collective logics behind the use of space and the environmental resources available (Ferrara et al. 2019). Century-old olive trees, on the island of Sicily



**Figure 1.** Century-old olive trees in Sicily, images taken from the ground. (a) A century-old olive tree located within the archaeological area of the temple Valley in Agrigento (ca. 5th century BC). (b) A century-old olive tree located within a house garden.

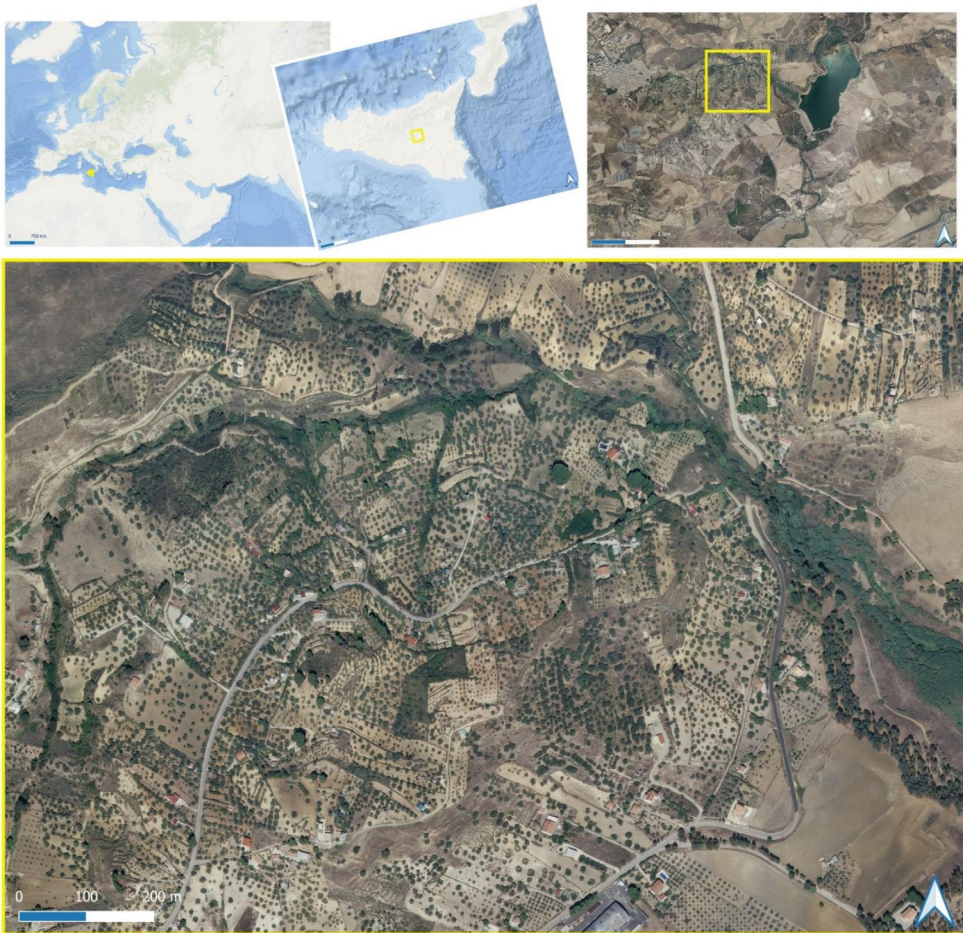


**Figure 2.** An example of different spatial configurations of the same land use, ‘olive groves’, classified as such by CORINE land cover. The location is a hilly countryside in Villarosa, a municipality in an inner area of Sicily (Italy). The image is the latest available RGB orthophoto (year 2013, pixel 25 cm, scale 1:10.000).

as elsewhere, as remnants of past vegetation in today’s landscapes present a unique scientific opportunity, since their diverse spatial configurations in themselves constitute an untapped source for understanding past land uses (Ferrara et al. 2019; Ferrara and Wästfelt 2021; Ferrara et al. 2024a). Their presence reflects the human configuration of space (Couclelis 2009), whose design is related to specific management practices depending on different historical periods, local temporal contingencies, land use activities and purposes (Howarth 2008; Couclelis 2009). In some occasions, such as the olive orchards present on the island of Sicily and explored in this paper, the spatial configurations of century-old olive trees have been robust enough in time to be distinguishable, even when changes in agricultural activities have brought relevant spatial changes in the environmental context.

We conceptualise spatial configurations of land use as geospatial objects, defined by their contexts and cognitively represented as **conceptual spaces** (Gärdenfors 2000; Ahlqvist et al. 2012). A conceptual space describes the structure of cognitive representations of the world (Gärdenfors 2000, 31). In simple words, a conceptual space is a description of how we mentally represent the properties and spatial structure (context) of,

for instance, an ‘old olive orchard’ (made of century-old olive trees, randomly sparse in the field), or a ‘fruit garden’ (made of fruit trees) or a ‘cereal field’ (made of cereal crops and no or few trees). A conceptual space is a theoretical cognitive entity that we construct and use to access epistemologically certain empirical phenomena. In this paper, the conceptual space ‘olive orchard’ is a cognitive entity that explains the observed many olive trees spatially arranged in certain ways. In simply words, a conceptual space is the epistemological bridge between the spatial dimension of the perceived reality and our mental representation of it as a concept. As historical agroecosystems/landscapes are characterised by complex structures that undergo constant reorganisation in multiple and diverse spatial arrangements, epistemologically these multiple and diverse spatial arrangements are traceable through conceptual spaces as mental representations of diverse land uses and/or land organisation spatial features.

In this paper, we continue the work done by Ahlqvist (2005) and Ahlqvist et al. (2012) on the application of the cognitive theory of conceptual spaces for the geospatial investigation of land cover and land use changes, progressing such methodological approach with the use of just one single image for the detection of land use changes. We ground on the assumption that diverse spatial configurations of olive trees still present today in historical olive agroecosystems are the simultaneous expression, in the present space, of diverse spatial and temporal dimensions of their land use. Shifts of spatial configurations related to land uses and functions over time can be reflected to a certain degree by the land cover and biophysical elements we see today, if some past spatial features have remained in present space. As spaces change over time, similarly do our mental representations of them. Our cognitive representations are not static, but change according to the context in which they are developed and used (cf. Gärdenfors 2000, 102). For instance, what we define today as ‘olive orchard’ may have had a different conceptual meaning in the past for locals. On a long-term temporal scale, an ‘olive orchard’ of today may thus partially or totally overlap with different past conceptual spaces (e.g. agroforestry, as exemplified by Figure 3). In other words, adopting a perspective based on conceptual spaces, we are able to realise that, for example, *the same space can be today an olive orchard, as well as, have remnants of a past agroforestry system* (cf. Figure 3 for a conceptual model of past-present transformations in a landscape today classified with the same land use).

Using a Sicilian landscape made of historical olive agroecosystems as case study, this paper demonstrates the possibility of mapping physical representations of past land uses and both their change and persistence dynamics in historical landscapes from a single Earth observation product. Such possibility relies, methodologically, on the analysis of category similarity (Ahlqvist 2005, 2008) between multiple classes that embody different conceptual spaces of the same land use. These classes are historically contingent geospatial contexts, extracted from an image through a supervised contextual post-classification technique we have developed (Ferrara et al. 2024a).

The paper is structured as follows. In the next session, we present the area chosen as case study. Section 3 details our geospatial method, applied here to analyse historical dynamics of the same land use from an orthoimage. The section presents also a cross-validation approach using plant microfossils (in the form of phytoliths) to test the reliability of our results for the interpretation of land use history in the study area. Section 4 describes the results of our analysis, showing the possibility of mapping, from a single Earth observation product, legacies of past spatial configurations of the same land use in today’s historical landscapes and their agroecosystems.

## From past to present

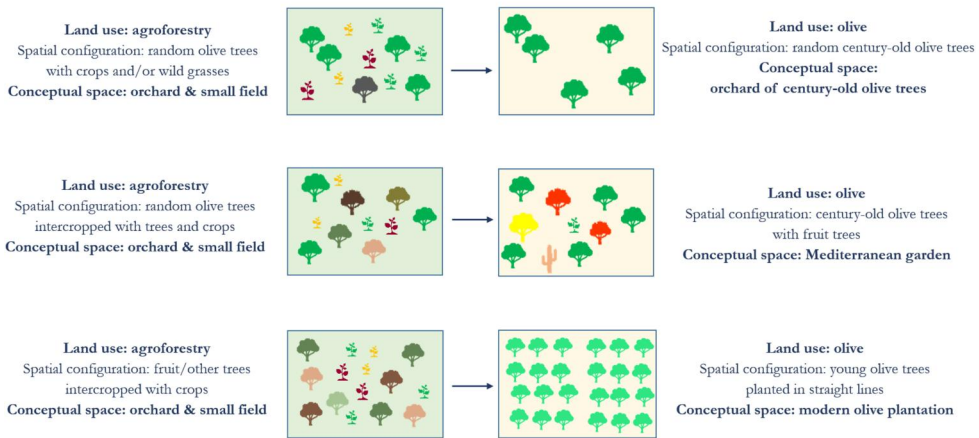


**Figure 3.** Conceptual model of past – present transformations in a landscape classified today with the same land use. The model shows how the same land use today (in this case the CLC class ‘olive growing’) may correspond to different spatial configurations of the same crop (for instance, orchards of century-old olive trees, Mediterranean gardens and/or modern olive plantations). The model shows how these different spatial configurations may correspond to a different land use of the same space in the past (e.g. agroforestry). As space where today we can see some remnants from these past uses (embodied by the big olive trees in green in the image).

In [Section 5](#), finally, we discuss how it is possible, with our geospatial approach applied to the analysis of a single image, to reach a higher level of understanding of the multitemporal dimensions of the use of the same space.

We conclude the paper by emphasising how an Earth observation product can become a multi-dimensional source of information that enriches our understanding of landscape changes and land use processes, with their underlying local ecological, cultural and social dynamics. As such, we show the potentialities of geospatial analysis in producing useful knowledge that can be applied in correlation with archaeological and archaeobotanical investigations of landscapes with a deep history.

## 2. Study area

Our study area represents a landscape where human-nature entanglements spanning over centuries and even millennia have resulted in remnants of century-old olive trees, today surrounded by other land uses, including intensive cereal cultivation and private countryside smallholdings for leisure ([Figure 2](#)).

This rural area of inner Sicily (N 37° 35' 7.3968, E 14° 11' 28.9824), part of the municipality of Villarosa (Enna province), lies in the middle of the Morello Valley, a past fluvial system inhabited since prehistory. The area depicted in the orthoimage under study in this paper covers approximately 21,46 km<sup>2</sup>. A mosaic of multiple and diverse olive spatial configurations are concentrated on the hill *Cozzo del Lampo*, as century-old olive trees in pocket terraces or scattered across the area, century-old olive trees intercropped with other fruit trees or with wild olives, and young olive trees planted in straight rows. These agroecosystems can be defined as Mediterranean formations of *Olea europaea* var. *europaea*, characterised by the presence of Mediterranean subnitrophilous grass communities (graminoid formations covering post-cultural or pasture lands), sub-Mediterranean deciduous thickets and diss formations. Along the slopes of the hill, these olive

agroecosystems are intermixed with Mediterranean tall-grasses, evergreen sclerophyllous scrubs and riparian thickets close to the small water streams. The hill is then surrounded by extensive annual cultivations of cereals (under a crop rotation system including fallow) and complex agricultural systems (formed by a mosaic of parcels with diverse land use types, from annual crops to pasture and/or permanent crops). Based on recent collection of oral histories and what we have elsewhere referred to as ‘geospatial narratives’ (Ferrara et al. 2024b), we know that until c. 1950 certain fruit trees (*Pyrus pyraster* L. (Burgsd.), *Punica granatum* L., *Prunus spinosa* L. subsp. *spinosa*, to name a few) were maintained in between the century-old olive trees, resembling thus an intercropping system.

Olive trees have been present in the case study area for several centuries (Ferrara 2016; Ferrara et al. 2022). These century-old olive trees are mainly located in places where it was difficult or impossible to plough and grow cereals. Being century-old, these trees constitute thus *ecocultural legacies* from past land uses into the present space. As we will argue here, even though this area is today characterised by different conceptual spaces of the same land use (olive growing), they are centred on the predominant presence of these ancient olive trees. In our approach, we have thus used the spatial arrangements of these century-old olive trees as ‘control points’, firstly to extract different conceptual spaces related to their land use and, secondly, to gain information on the diverse temporal and spatial dynamics of such use over the long term (as further explained below, cf. Section 3.1).

Within the Vetenskapsrådet research project ‘The Biocultural Heritage of Sicilian Olive Trees’ (Ferrara 2024), in 2022 and 2023 archaeobotanical excavations in old olive orchards of the area have been undertaken to reconstruct *in situ* past vegetation dynamics and land use history using phytoliths analysis (i.e. biogenic silica plant microfossils). In this paper, the results of phytoliths analysis are used to cross-validate if our geospatial methodological approach is suitable to investigate the land use deep history of a site.

### 3. Methods

#### 3.1. Category similarity in temporally different contexts of the same land use

Over four decades ago, Butzer (1980) argued that archaeologists need to recognise how communities in the past interacted spatially, economically and socially with the environment they were living in. Consequently, there was a need for a multiscale and multidimensional contextual method in ecological approaches to the past. A few years later, Hodder (1985) proposed that spatial archaeology should focus on the identification and study of contexts. The aim was *to read meanings* through two main lines of enquiry: the consideration of the environmental and behavioural context, as well as a look at the networks of associations objects were placed within.

Hodder and Hutson (2003) defined the context of an archaeological attribute as the totality of the relevant environment, or the relationships that the object has with its environment, an understanding necessary for discerning the meaning of the object itself. From archaeology, it became clear that people, places and material culture are all linked together in a relational network of meanings within the landscape. Even though the spatial context may work to stabilise meanings, these meanings are never permanent. Nonetheless, they are located in space as imprints and, because of this, contexts can be both analytically specified and investigated (Dixon and Jones 1998).

Crossing the bridge between time and space, Carole Crumley similarly emphasised the importance of the correlations between spatial arrangements of landscape and

environmental elements in time, whose analysis may enable further pattern recognition at any spatial scale and reflect both distant and recent history of human-environment interactions (Crumley 1979; Crumley 2000). We follow such thread on the importance to take into consideration the contextual dimension of spatial objects in a landscape. In this paper, we apply our supervised contextual post-classification method (Ferrara et al. 2024a) to extract, from a single Earth observation product, geospatial objects (classes) that represent temporally different conceptual spaces of the same land use within a historical landscape. We then analyse the degree of (semantic) category similarity between these classes to gain insight into dynamics of change and persistence of that land use over time.

Our method builds on previous work on spatial relational post-classification (Wästfelt 2009; Ahlqvist et al. 2012; Wästfelt and Arnberg 2013; Wästfelt 2015). This method allows to map different social-spatial distributions of land uses from the same land cover, by using the spatial context of pixels (cf. Gurney and Townshend 1983) as an integrative source of information to refine and improve classification results. Gurney and Townshend (1983) list four basic forms of spatial contextual relationship (distance, direction, connectivity and containment). In our work, we have chosen the largest nearest neighbour (Euclidean) distance between the pixels in the training area (Wästfelt 2009), as a spatial relation that defines and measures the context of a pixel.

In recent work (Ferrara and Wästfelt 2021), we have shown how unsupervised spatial-relational analysis based on contextual criteria (Nielsen et al. 2014; Nielsen 2015) can be applied to extract, from a single image, classes carrying information on the multiple historical, cultural and ecological processes of a heterogeneous landscape. The method applied in this paper is the supervised version (Ferrara et al. 2024a) of the same geospatial approach. In our method, a conceptual space such as, for instance, ‘intensive orchard of crop  $x$ ’ is categorised in terms of its geospatial context. A geospatial context refers here to peculiar spatial configurations defined by the contextual relationships among its constitutive elements, in terms of biophysical features, human-nature processes, intentionalities and ecological dynamics. A conceptual space categorised as context is then computed as a training area, used to set the clustering conditions of a supervised classification routine of the entire image data (Figure 4).

Computationally, our method is operationalised by *CS.py*, a plugin for the Open-Source Geographical Information System program QGIS, written in Python programming language (Ferrara et al. 2024a). With *CS.py*, it is possible to use training areas, defined by the user, to identify and extract in the image data conceptual spaces whose spatial contexts have the same spatial features present in the training areas. In our method, each training area represents a conceptual space related to a local spatial configuration and the contextual relationships among its constitutive elements. In simple words, the training area is the computational embodiment of the geographical context in its spatial and temporal semantics.

The supervised contextual post-classification procedure automated by *CS.py* consists of two analytical phases: 1) a **training phase** and 2) a **contextual post-classification** phase. In the **training phase**, the portion of the input (pre-classified) image corresponding to the training area (defined by the user as expression of a conceptual space) is taken into consideration. The aim of this phase is to define the training area (spatial) criteria to use for the contextual post-classification of the entire input image (which will be done in the step afterward).

In this phase, initially, for each of the pixels of the input (pre-classified) image, the so-called ‘contextual feature vectors’ are calculated (cf. feature vector calculation flowchart in Ferrara et al. 2024a). The contextual feature vector contains information about the



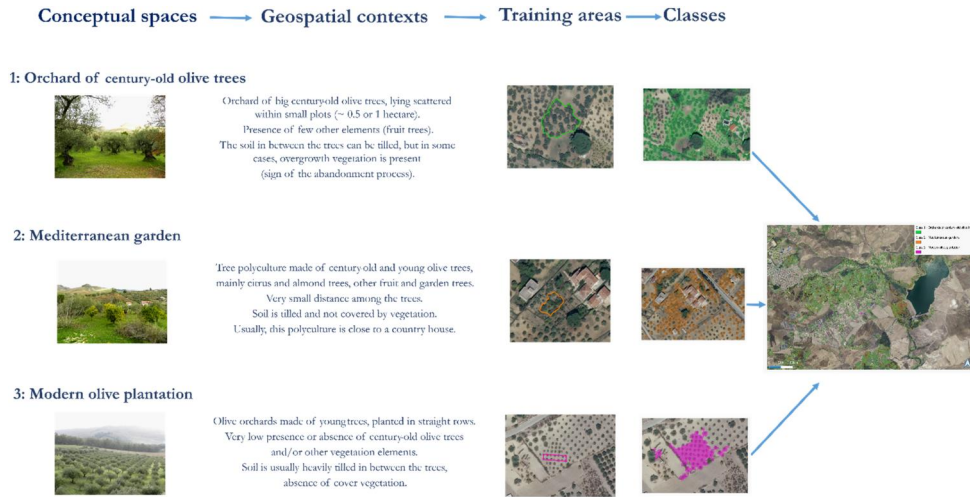


**Figure 4.** Three different conceptual spaces of the same land use ('olive growing'), extracted as geospatial contexts (classes) and validated in Ferrara et al. (2024a) from an RGB orthophoto of the study area.

pixel's surroundings, specifically each pixel's geometric (Euclidean) distance (nearest-neighbour distance) from each pixel to all the nearest pixels of all the different classes present in the pre-classified input image. In our methodological approach, calculating the nearest-neighbour distance is a computational way to describe the contextual surroundings for each pixel. It follows now the proper training phase, in which our algorithm calculates the spatial-contextual criteria from the training area defined by the user. The contextual information used as a spatial criterion is the *largest nearest neighbour distance* (Wästfelt 2009). The largest nearest neighbour distance (or the smallest nearest distance able to cover the largest area) is calculated by first calculating all nearest neighbour values between all the pixels of the classes in the training area, and secondly by keeping only the largest for each neighbour relation.

In the **contextual post-classification phase**, our algorithm uses the spatial-contextual criteria calculated in the previous training phase to re-classify each and every pixel in the input image according to these criteria and their contextual feature vectors (calculated in the previous phase as well). In this post-classification procedure, every pixel having a spectral class represented in the training area is evaluated based on its nearest neighbour (Euclidean) distance to different spectral classes (information stored in the contextual feature vectors) and the largest nearest neighbour distances calculated for each pixel in the training area. If a pixel outside of the training area has the same spectral values of a pixel inside the training area, but has a nearest neighbour distance larger than the largest nearest neighbour distance found in the training area for that spectral class, it will be classified as having a different spatial context compared to the pixels of the training area. In other words, even though this pixel has the same spectral class as another pixel in the training area, it is classified as a different feature because of its different spatial context (i.e. its nearest neighbour distance is larger than the largest nearest neighbour distance found in the training areas for that spectral class). Only pixels having a spatial context corresponding to the spatial context of the pixels in the training area are considered indicative of on-the-ground features similar to those embodied in the training area. In Ferrara et al. (2024a), the reader can also find a description of the four preliminary steps needed to prepare the input image and the training areas for the analysis, as well as the post-processing stage.

To map and interpret the history of land use changes from the image of our study area (Figure 2), we worked with three different conceptual spaces of the same land use ('olive growing', CLC), which represent different types of olive cultivation related to different land use logics and management practices in time: 1. Orchard of century-old olive trees; 2. Mediterranean garden; 3. Modern olive plantation (Figure 4, left side). The orchard of century-old olive trees (Conceptual space 1) is today a remnant of a typical past agroforestry system, where olive trees were scattered and mixed with other crops (e.g. legumes and cereals) and fruit trees (e.g. pear, pomegranate, almond and prunus) and/or used for grazing (Ferrara et al. 2023). For Mediterranean garden (Conceptual space 2), we intend here both century-old and younger olive trees intercropped with other fruit trees (mainly young citrus and orange trees), in small plots usually located in the gardens of country houses. A modern olive plantation (Conceptual space 3) is characterised by the presence of a high density of young olive trees and no other vegetation features, planted in rows close to each other, usually on plain terrains, so to facilitate harvest and tilling. It is important to notice that these three conceptual spaces respond to different timescales of the same land use. Based on local geonarratives and change analysis done on historical aerial images (cf. Ferrara et al. 2024b), we know that the century-old olive orchards (age unknown) are older than the fruit gardens attested at least from the 1950s (Ferrara et al. 2024b) and that the fruit gardens are older than the modern olive plantations (from 1990s).

These three diverse conceptual spaces of the land use 'olive growing' have been extracted as geospatial contexts (classes) from an RGB orthophoto of the study area, year 2013, 25 cm pixel resolution, scale 1:10.000 (Figure 4, right side) (cf. Supplementary material available in Ferrara et al. 2024a).

To map and interpret land use changes over time in the image of the study area, we performed a correspondence analysis among these three different classes of the same land use (Figure 4). We first calculated and validated the area of spatial overlap among these conceptual spaces/classes, and then we analysed their different degrees of overlap depending on the direction of the overlap (i.e. being the overlap area between Class 1 and Class 2 the same, if Class 1 overlaps Class 2 we will have a certain degree of overlap which will be different if Class 2 overlaps Class 1).

To perform the correspondence analysis, we used the **Overlap Analysis algorithm in QGIS**,<sup>1</sup> which calculates the area and percentage cover by which features from an input layer are overlapped by features from selected overlay layers. The Overlap Analysis gives as a result an output layer with new attributes, reporting the total area of overlap and the percentage of the input feature overlapped by each of the selected overlay layers. We calculated the correspondence among the three olive land use classes extracted from the input image with our supervised contextual post-classification method (Figure 4), in order to analyse their overlaps as degrees of category similarity, re-adapting Ahlqvist's (2008) overlap analysis approach done for heterogeneous land cover classes. Specifically, we performed an overlap analysis between Class 1 (Orchards of century-old olive trees) and Class 2 (Mediterranean gardens), and between Class 1 and Class 3 (Modern olive plantations), with the aim of understanding the spatial correlation between century-old olive trees (geospatial context 1) and geospatial contexts that have more recent spatial configurations of vegetation features (geospatial contexts 2 and 3).

The idea to investigate overlapping dynamics allows for detecting and interpreting more than one single temporal dimension of land use from present space. Mapped overlaps are the spatial expression of the temporal transitions between past and present land

uses, where something from the past land use has remained in present space (thus the overlap surface). These computational overlaps detected between geospatial objects are the access key to map dynamic land use practices. Overlap allows the possibility to map past land use in present space and, most importantly, how it has turned into another use of the same space. Today, for instance, we can see a garden with both young fruit trees and a few century-old olive trees. The old olive trees (remnants of past land use) and the younger fruit trees are thus occupying the same space, but they represent different temporal scales of land use. However, since some spatial features of the past land use (the old olive trees) have remained in the present orchard, the past use of that land overlaps to a certain degree with the present use of the same space. Such overlap has been defined by Ahlqvist (2005, 2008) as category similarity in semantic terms, in the sense that a spatial object can simultaneously represent different categories of land use, in this case being - for instance - both today's garden and past orchard.

The accuracy of the output layers mapping the areas of overlap between the above mentioned classes has been validated using the F1 score as a metric. In remote sensing, the error matrix approach is the standard validation method of land cover and land use products (cf. Foody 2008). In the case of our results, a standard error matrix cannot be performed to validate the classification accuracy since the pixels forming the overlap areas belong to two different classes at the same time (e.g. in the case of overlap between Class 1 and Class 2, then the pixels forming the overlap area belong both to Class 1/Conceptual space 1 and to Class 2/Conceptual space 2). Nonetheless, even though we do not have classes that exclude each other, we can still adopt a binary approach for the sake of validation and consider the overlap area as one class and the no-overlap area as another class. As such, in order to validate the robustness of our overlap analysis, we tailored the standard method applied in object based analysis, the calculation of the F1 score (cf. Alias et al. 2018; Gao and Li 2019; Zapata-Pérez et al. 2020), to validate the presence or absence of just one class representing the overlap areas (cf. Soubry et al. 2022 for similar validation method).

The result of our Overlap Analysis is a set of polygons that outlines all overlapping areas between the classes extracted from the input image. The accuracy of such overlaps was done using a confusion matrix computed using as validation ten different data sets of random points that correspond to the reality in the field. The random distribution of sampling points must be as much representative as possible of the entire classified area (cf. Van Genderen et al. 1978; Thomas and Allcock 1984). Consequently, ten rounds of 200 random points each, generated at a minimum distance of 10 metres between each other within the layer extent of the overlap area, have been used as validation dataset. Crews-Meyer et al. 2004 argue that, in case of high resolution input images showing sufficient details to derive reference data with high certainty, random points as secondary independent dataset can be considered as absolute ground truth when visually inspecting the image. Furthermore, our choice to generate random points as validation dataset responded to the need to reduce the subjectivity in the identification of the validation points used for accuracy assessment (*sensu* Gromny et al. 2019 in Belcore et al. 2020).

By computing in a confusion matrix the presence and/or absence of the classified overlap with the presence and/or absence of real overlap in the location of the random points (Table 1), it is possible to compare the number of True Positives - TP (classified overlap areas that match overlap in reality), False Positives - FP (classified overlap areas that do not correspond with overlap in reality) and False Negatives - FN (overlap areas that exists in reality but that our classification has failed to detect as such).

**Table 1.** Confusion matrix created and used to validate the accuracy of the overlapped areas mapped.

		Validation points	
		Presence	Absence
Overlap area	Presence	<b>True Positive- TP</b> (The mapped overlap is observed in reality)	<b>False Positive- FP</b> (The mapped overlap is not observed in reality)
	Absence	<b>False Negative- FN</b> (The overlap observed in reality is not mapped)	<b>True Negative- TN</b> (No overlap neither mapped nor in reality)

From the confusion matrix, it is possible to measure the precision  $P$  and the recall  $R$  of the detections, necessary for the calculation of the F1 score to quantify the accuracy of the image analysis (cf. Padilla et al. 2020; Mehmood et al. 2022).

Precision is the ability to identify only relevant objects (correct positive predictions), calculated as the ratio of the number of true positives to the total number of predictions (Yang et al. 2020; Shi et al. 2022):

$$\text{Precision} = \frac{TP}{TP + FP} = \frac{TP}{\text{all detections}}$$

Recall is the ability to find all relevant cases (all ground-truths), calculated as the ratio of the number of true positives to the total number of actual (relevant) objects (Shabbir et al. 2021):

$$\text{Recall} = \frac{TP}{TP + FN} = \frac{TP}{\text{all ground truths}}$$

The weighted average of Precision and Recall is the F1 score, calculated to quantify how well an image analysis succeeds in detecting true objects existing in reality (overlap areas in our case). The F1 score values range from 0 to 1, with 1 means highest accuracy.

$$\text{F1 score} = \frac{2 * (\text{Precision} * \text{Recall})}{\text{Precision} + \text{Recall}}$$

We then estimated the uncertainty relative to such accuracy by calculating a confidence interval (CI, reported at 95%) for the relative error between the mapped overlaps (True Positive + False Positive) result of our contextual post-classification method and the observed overlaps (True Positive + False Negative) given by the random points as validation dataset.

Once we validated the accuracy of the classified overlaps, we specifically analysed the results of the overlap analysis in terms of the percentages of each overlap. We focused on the degrees of overlap between Class/Conceptual space 1 (Orchard of century-old olive trees) and Class/Conceptual space 2 (Mediterranean garden), and between Class/Conceptual space 1 and Class/Conceptual space 3 (Modern olive plantation). Our aim was to understand better the correlation in space between century-old olive trees (Conceptual space 1) and conceptual spaces more recent in time (Conceptual spaces 2 and 3). Our methodological approach takes into account **the key informative aspect** that two geospatial objects overlapping each other have different degrees of overlap and exactly these different degrees of overlap are informative to understand spatial change dynamics and thus to trace – partially and from a single image – the local land use history. The reason why two geospatial objects overlapping each other to a certain degree have different degrees of overlap depends on *the direction of the overlap analysis* (cf. Ahlqvist 2008). In

simply words, the overlap between century-old olive tree orchards over Mediterranean gardens represents the percentage of the pixels classified as century-old olive orchards (Conceptual space 1) that occupy the same space of the pixels classified as Mediterranean garden (Conceptual space 2). The overlap between Mediterranean gardens over century-old olive orchards represents instead the percentage of the pixels classified as Mediterranean garden (Conceptual space 2) that occupy the same space of the pixels classified as century-old olive orchards (Conceptual space 1). In other words, the same physical space, where the two conceptual spaces overlap, corresponds to different percentages (degrees) of overlap, depending on the direction we are looking at the two spatial objects overlapping (if, for instance, Conceptual space 1 is overlapping over Conceptual space 2, then the overlapping surface is the percentage of Conceptual space 1 overlapping over Conceptual space 2. If, instead, Conceptual space 2 is overlapping over Conceptual space 1, then the overlapping surface represents the percentage of Conceptual space 2 overlapping over Conceptual space 1. Cf. [Figure 8](#) for clarification).

The possibility to map degrees of category similarity among geospatial objects (classes), in our case expressed by the percentage of overlap areas, is what allows us to catch land use temporal dynamics within a single image data. By mapping degrees of overlap between different spatial configurations of century-old olive trees in the same space, in this paper we intend to verify if it is possible to map the temporary and transient conjunctures of different conceptual spaces depicted in the digital image. The physical conjunctures in space between part of a century old olive orchard and part of a Mediterranean garden (in other words, the possibility that there are some fruit trees in an old olive orchard and some old olive trees in a fruit garden) can tell us more about how these two different land use practices are correlated and depending on each other through time. In simply words, such mapped conjunctures can be informative about what has caused the patterns observed today.

### **3.2. Land use history from plant microfossils**

Our overlapping areas represent the conjunctures in space between different spatial objects (classes) corresponding to diverse temporalities of land use, as explained above. To further cross-validate if these mapped spatial configurations are informative on past land use and vegetation dynamics in a historical site, we compared the results of our overlap analysis with independent evidence derived from plant microfossils (phytoliths) analysis done in the same study area. Our choice of the use of phytoliths for cross-validation is justified by the lack of geospatial data or other datasets and/or archives that can be temporally related to the onset of Class/Conceptual space 1, whose century-old olive trees may be at least older than 500 years (cf. proposed different ages for similar trees elsewhere in Sicily by [Schicchi and Raimondo 2011](#); as elsewhere in the Mediterranean by [Arnan et al. 2012](#), [Cherubini et al. 2013](#), [Urwin 2013](#), [Bernabei 2015](#), [Camarero et al. 2021](#), [Camarero et al. 2024](#)). In other words, the methodological approach that we propose here is to validate the diverse temporalities of the same land use mapped with our geospatial approach with in-situ land cover and land use change reconstructions based on plant microfossils. Furthermore, we wanted to test the potential suitability of combining geospatial analysis with archaeobotanical evidence, to assess if such a procedure could enrich our knowledge about landscape with a deep history of human-nature interactions.

Phytoliths are plant microfossils in the form of biogenic silica that remain preserved, when all the organic components of a plant decay ([Pearsall 2015](#)). Present in the soil underneath the landscape we see from an image, the study of phytoliths morphologies

and assemblages can be used to reconstruct past vegetation patterns and dynamics (Pearsall and Trimble 1984; Strömberg et al. 2007; Aleman et al. 2014; Feng et al. 2017). The extraction method isolates a maximum quantity of phytoliths from soil and sediment samples (cf. Mazuy et al. 2024 for details on the extraction protocol). Phytoliths have been sampled in five soil stratigraphic profiles distributed over the study area. In this paper, we have included as cross-validation evidence the results from phytoliths analysis done in two stratigraphic profiles 1.5 m deep (Figure 5), where soil was sampled every 10 cm, resulting in 30 samples, whose phytoliths are here used as cross-reference material (Supplementary material 1). We call these profiles A and B. Three pieces of charcoal from Profile A were submitted for radiocarbon dating, carried out at the Ångström Laboratory – Radiocarbon group at Uppsala University. Dates were calibrated directly by the laboratory using IOSACal v0.4.1 and the IntCal20 calibration curve (Reimer et al. 2020) (Supplementary material 2a), and a Bayesian age-depth model was produced in R (R Core Team 2021) based on the uncalibrated dates using the package Bacon (Blaauw et al. 2022) (cf. Supplementary material 2a and 2b).

Phytolith extraction was undertaken at the Palaeobiology Laboratory (Department of Earth Sciences and Uppsala Archaeobotanical Group, Uppsala University) and the interpretation of results took place at the UMR 7264 CE-PAM CNRS-Université Côte d’Azur (Nice, France). A minimum of 200 diagnostic morphotypes of phytoliths (Figure 6) every 10-cm stratigraphic layer per each profile were identified and categorised into plant taxonomic groups according to the International Code for Phytolith Nomenclature (ICPN) (Neumann et al. 2019), reference literature and the PhytCore online database,<sup>2</sup> and counted using light microscopy at  $\times 400$  magnification.

Each morphotype’s relative abundance per profile was then calculated, and assemblage analysis performed by comparing different morphotype proportions with distribution

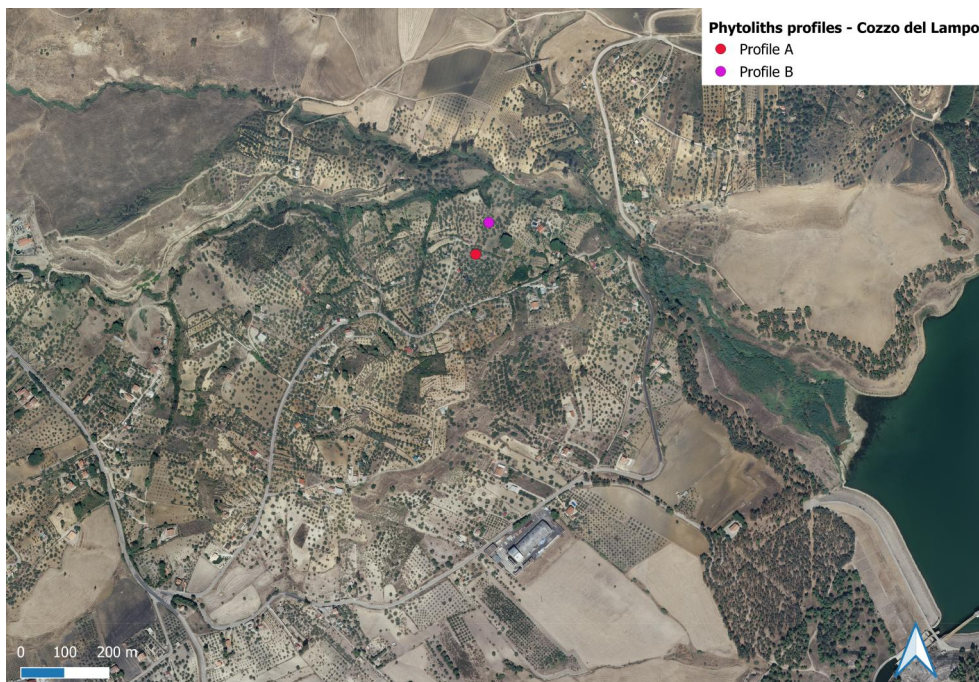


**Figure 5.** Location of profiles A and B opened for soil sample collection and phytolith analysis in the study area.

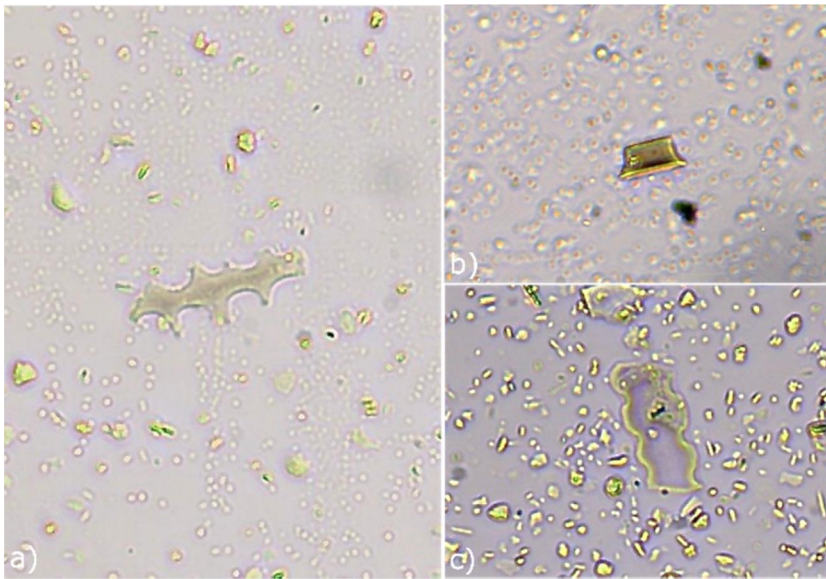


**Figure 6.** Phytoliths extracted from the two stratigraphic profiles excavated in the study area and used in this paper as cross-validation. (a) Elongate dentritic phytolith morphotype from profile A layer 1-20 (20 cm depth); (b) rondel phytolith morphotype from profile A layer 1-30 (30 cm depth); (c) crenate phytolith morphotype from profile B layer 1-40 (40 cm depth). Scale 40  $\mu\text{m}$ .

curves of four calculated indices: the *Dicots/Poaceae index*, the *long/short cell index*, the *inflorescence/culm-leaves index* and the *Fs-index* (cf. [Supplementary material 3](#)).

Out of these four indices used in the phytoliths analysis, the most relevant for the cross-validation of our results from the overlap analysis is the trees vs grasses index or *Dicots/Poaceae index* (referred to here as the D/P index). The D/P index measures the ratio of dicotyledons rough- and smooth-spherical morphotypes (D) diagnostic of trees and shrubs versus Poaceae morphotypes (P) diagnostic of grasses. By calculating the ratio of trees (D) to grasses (P), the D/P index allows thus to estimate tree cover density (Alexandre et al. 1997). The lower the D/P value, the more open the habitat since the proportion of phytoliths from grasses is higher compared to dicots phytoliths. The D/P index is based on the assumption that the presence of grass phytoliths in the soil of open habitats is higher than phytoliths from trees and/or shrubs (Strömberg et al. 2018). Delhon et al. (2003) use 0.1 as the lower limit in the D/P value to distinguish between dicotyledon- versus grass-dominated environments in Mediterranean contexts.

In this paper, the D/P index is considered informative about the different classes/conceptual spaces of olive land use (cf. [Section 3.1](#)), since these classes are based on the spatial arrangements of trees (thus also their density) and their geospatial contexts in terms of different degrees of habitat openness (which can signify, for instance, the presence of intercropped trees or grasses or bare soil). As such, the analysis of the phytolith records along the soil layers of a stratigraphic profile can be informative of the land cover and land use history of the geospatial context where that profile has been excavated. For example, a soil layer having phytolith records showing a grass-dominated environment will indicate the presence of an open habitat and grasses among the (olive) trees, at the time of that soil layer formation. Within the same stratigraphic profile, another soil layer (thus formed temporally in a different phase) dominated by dicots phytoliths will be then indicative of a different geospatial context, characterised by a higher presence of trees, thus indicative of intercropping land use practices.

The other indices used in the phytolith analysis have provided complementary information. The *long/short cell index* measures the ratio of long cells (formed in mature grasses, cf. Rencheng et al. 2017) vs short cells (formed in young grasses, cf. Sangster 1970), explaining thus grass composition in a field (mature versus young grasses) at the time of deposition in the soil (Delhon et al. 2024). The *inflorescence/culm-leaves index* measures the ratio of phytoliths from inflorescence bracts versus phytoliths from culms and leaves (Piperno 1988). A high presence of inflorescence phytoliths indicate the presence of mature plants with spikelets (ready to be harvested), being informative about seasonal agricultural practices (e.g. harvest) or cereal processing (Delhon et al. 2020). The *Fs-index* (Bremond et al. 2005, 2008), based on the presence of bulliform flabellate phytoliths (formed after the leaf-rolling response to water stress, cf. Bremond et al. 2005; Mader et al. 2020), provides information on microhabitats and local climatic conditions.

Vegetation reconstructions based on phytolith records, covering several millennia, can thus trace the land cover and land use history of a geospatial context. In this paper, we adopted such method to trace the land use history of some of the conceptual spaces mapped in the previous steps and gain more information on their overlapping dynamics.

## 4. Results

### 4.1. Past land use changes traceable in present space

The three diverse classes of olive land use extracted and mapped with *CS.py* (Ferrara et al. 2024a; Figure 4) represent how people arranged and used the local space over time, as each of these spatial configurations corresponds to different temporalities as clarified in 3.1.

By mapping their overlap areas and calculating the degrees of respective overlap among these different spatial configurations of century-old olive trees in the same space, we have been able to map the *conjunctures* between the different geospatial contexts extracted and classified in the digital image. Figure 7 shows examples of the spatial conjunctures between Class 1 ‘Orchards of century-old olive trees’ and, respectively, Class 2 ‘Mediterranean gardens’ on the left and Class 3 ‘Modern olive plantations’ on the right.

The total area of overlap between Class 1 and Class 2 is 1,066 km<sup>2</sup>, while the total area of overlap between Class 1 and Class 3 is 0,078 km<sup>2</sup>.



**Figure 7.** (a) Examples of spatial conjunctures (overlaps) between Class 1 ‘Orchards of century-old olive trees’ (in green) and Class 2 ‘Mediterranean gardens’ (in orange), and (b) between Class A ‘Orchards of century-old olive trees’ (in green) and Class 3 ‘Modern olive plantations’ (violet).



The calculated respective degrees of overlap between Class 1 and Class 2, and between Class 1 and Class 3 are shown in [Table 2](#) below.

The result from the overlap analysis between Class 1 (Orchard of century-old olive trees) and Class 2 (Mediterranean garden) is 7.5%, while the reverse overlap between Class 2 and Class 1 is equal to 76.6% ([Figure 8](#) for a spatial model explaining the overlap analysis and its bi-directionality). These results signify that the area of orchards made of century-old olive trees that has turned/changed into Mediterranean garden represent the 7.5% of the entire surface in the study area covered by orchards of century-old olive trees. At the same time however, this surface represents the 76.6% of the entire surface of the study area where Mediterranean gardens are present.

The overlap between Class 1 (Orchards of century-old olive trees) and Class 3 (Modern olive plantations) is very low (7.9%), while the reverse overlap between Class 3 and Class 1 is higher (26.6%). The results indicate that the presence of orchards made of century-old olive trees among new olive plantations represent only the 7.9% of the entire surface of the case study area where these ancient orchards are present. Nonetheless, the same surface represents the 26.6% of the overall surface classified as Modern olive plantation in the study area.

Results from the validation of the accuracy of our overlap analysis indicate that the mapped overlap area between Class 1 and Class 2 has an average F1 score of 0.68, with a mean relative error of  $-0.11114$  and a margin of error of  $\pm 0.14933$  with a sample size of 10 at confidence interval of 95%. The mapped overlap area between Class 1 and

**Table 2.** Degrees of overlap calculated, respectively, between Class 1 and Class 2, and between Class 1 and Class 3.

Degrees of overlap	Class 1 Century-old olive orchard	Class 2 Mediterranean garden	Class 3 Modern olive plantation
Class 1 Century-old olive orchard	100%	7.5%	7.9%
Class 2 Mediterranean garden	76.6%	100%	/
Class 3 Modern olive plantation	26.6%	/	100%

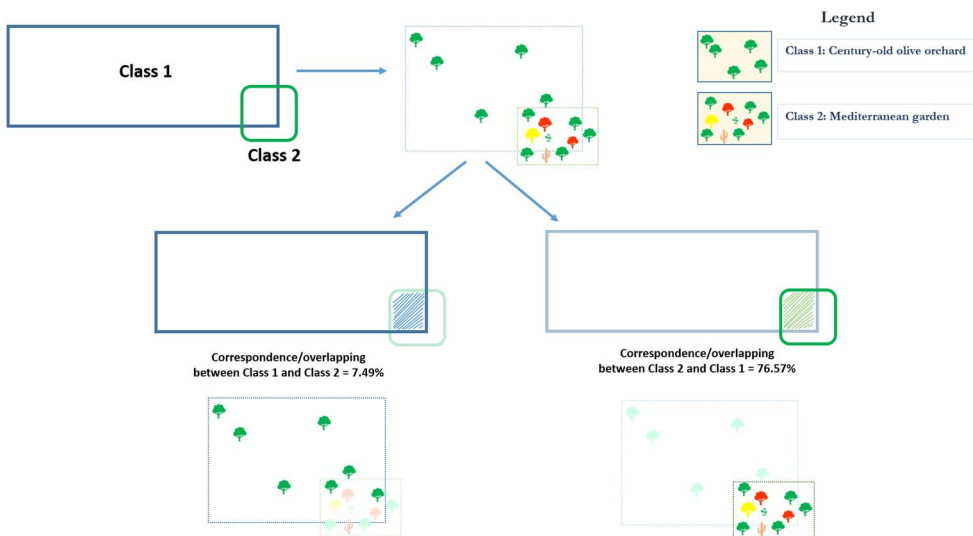


**Figure 8.** A spatial model explaining the results of the overlap analysis done between Class 1 (Orchard of century-old olive trees) and Class 2 (Mediterranean garden), in both directions of correspondence (sensu [Table 2](#)), in order to visually show the different degrees (%) of category similarity.

**Table 3.** Average F1 score and mean relative error (CI 95%) of the mapped overlap areas (Class 1 – Class 2, Class 1- Class 3).

	Average F1 score	Mean relative error +/- margin (CI 95%)
Overlap area Class 1 – Class 2	0.683673761	– 0.11114 +/- 0.14933
Overlap area Class 1 – Class 3	0.597142857	– 0.50333 +/- 0.163068

Class 3 has an average F1 score of 0.59, with a mean relative error of  $-0.50333$  and a margin of error of  $\pm 0.163068$  with a sample size of 10 at confidence interval of 95% (Table 3).

The F1score of 68% for the overlap between Class 1 and Class 2 and of 59% for the overlap between Class 1 and Class 3 can be considered as substantial, given the range of values of the F1 score within 0 to 1. Even though in the literature an accuracy of 85% is recommended as acceptable for land cover and land use classifications (Anderson et al. 1976 in Pan et al. 2022), Foody (2008) found that accuracy with 85% is difficult to obtain for many mapping applications. Furthermore, accuracy assessment values depends also on the characteristics of the site, the quality of the image, as well as the categories of classes mapped that need to be validated. Therefore, no standard accuracy values for land cover and land use classification can be appropriate for all study cases. The results of our validation demonstrated that the overlaps mapped have an accuracy over the average values, thus as such these classes have been analysed further in their overlapping behaviours.

#### 4.2 Crossvalidation with plant microfossils

The three classes we extracted and analysed in this paper (Class 1. Orchard of century-old olive trees; Class 2. Mediterranean garden; Class 3. Modern olive plantation) represent different histories of the same land use, which overlap to a certain degree in present space. From previous work, we know that the century-old olive trees present in the study area are older than the current fruit gardens and/or the modern olive plantations (Ferrara and Wästfelt 2021; Ferrara et al. 2024b).

We cross-validated our geospatial analysis with results from an independent phytolith analysis done in two stratigraphic profiles, excavated and investigated in an orchard with century-old olive trees and some sparse fruit trees, present – as many other similar orchards - in the case study area.

Profile A is located in an open area surrounded by century-old olive trees, not included in any of the classes extracted by our geospatial method. Profile B is surrounded by century-old olive trees (and a few fruit trees, old varieties of pear mainly, at a distance), classified by our method as Class 1 (Orchard of century-old olive trees), at very close overlap with Class 2 (Mediterranean garden) (Figure 9).

The cross-validation is based on the phytolith trees vs grasses D/P indices (Figure 10). The D/P indices curves in Profile A suggest an original semi-open habitat, resembling a shrubland-type of environment naturally expanding between approx. 4849–2871 BC according to the age-depth model we generated, which has then transitioned, along the millennia, into the few trees we see around the location today.

The progressive openness of this local context, indicated by the D/P indices, is substantiated from approximately AD 576 until today by the other indices used for the phytolith assemblage analysis. The *long/short cell index* curve shows a transition in the use of the local space from the progressive reduction of mature grasses to an increase in grasses cut

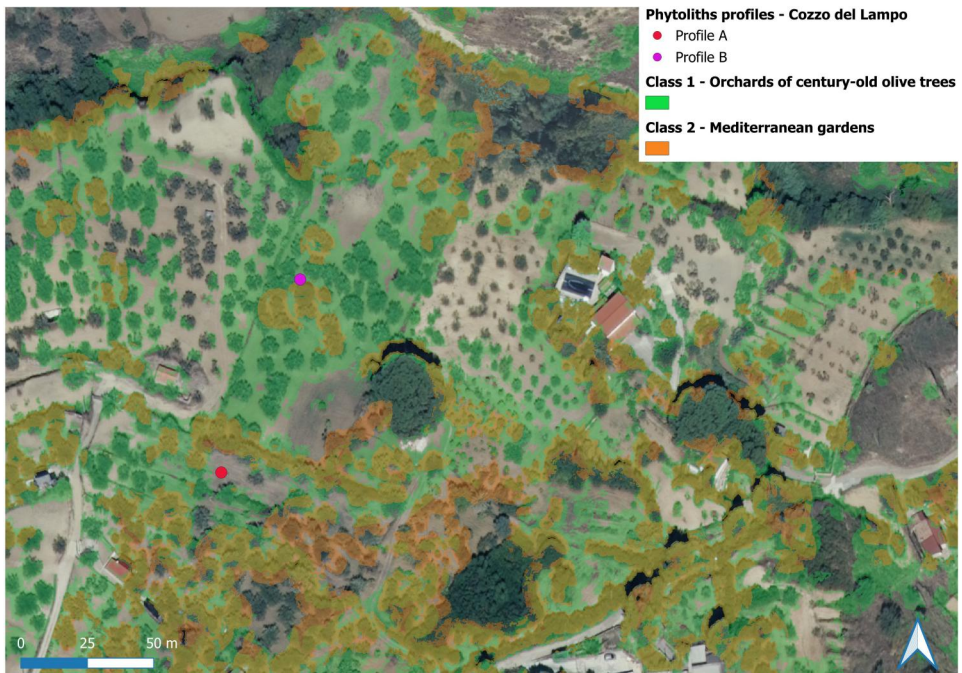


**Figure 9.** Location of the two profiles A and B opened for phytolith analysis in the study area, shown in the local space classified as Class 1 (Orchards of century-old olive trees, in green) and/or Class 2 (Mediterranean gardens, in orange).

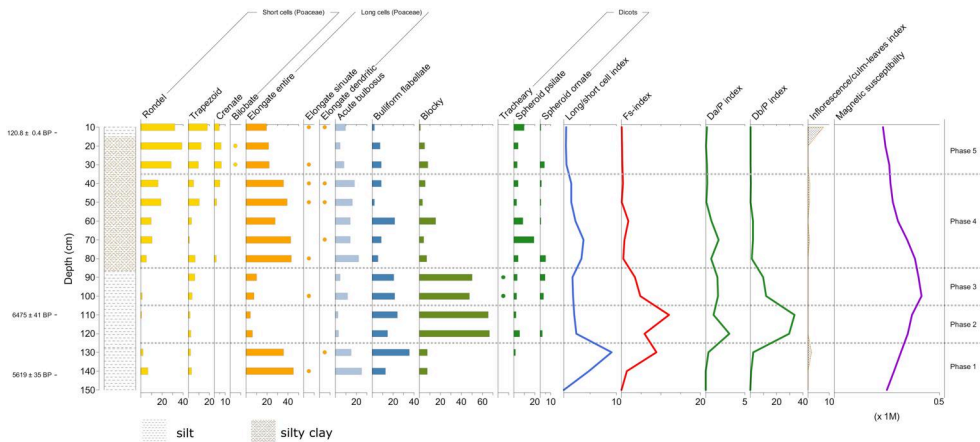


**Figure 10.** Phytolith diagram showing percentages of morphotypes from Profile A (yellow: grass phytoliths; green: dicots phytoliths) (dots indicate morphotypes < 1%). Inflorescence/culm-leaves index shown with exaggeration factor (60x). Note the difference in scale between the indices.

in their young stages, potentially sign of a change in grazing practices or other land uses (e.g. meadowing, modern tilling). Such progressive canopy openness along the entire profile until the uppermost part (cf. D/P indices curves in Figure 11), can be correlated with the area neither classified as Class 1 (Orchard of century-old olive trees) nor Class 2 (Mediterranean garden) by our geospatial method.

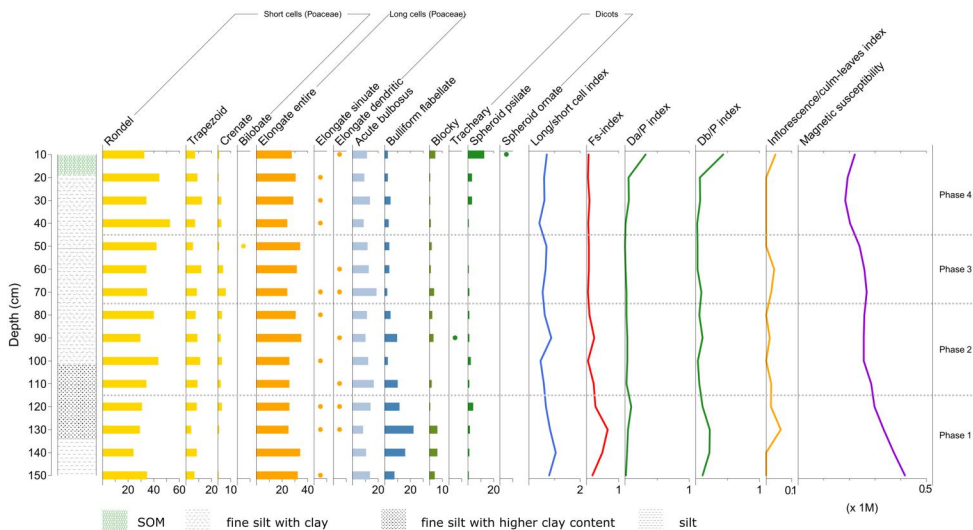


**Figure 11.** Phytoliths diagram showing percentages of morphotypes from Profile B (yellow: grass phytoliths; green: dicots phytoliths) (dots indicate morphotypes < 1%). Note the difference in scale between the indices.

Profile B has no absolute chronology available; it is classified as Class 1 (Orchard of century-old olive tree) and in close overlap with Class 2 (Mediterranean garden). The phytolith diagram (Figure 11) shows the passage from a woody/shrub environment to a more open environment (from Phase 1 to Phase 3), followed by a more recent steady increase in the presence of dicots (Phase 4, cf. D/P indices). The older temporal phases of the profile (Phase 1 and Phase 2) record mature grasses (cf. *Long/short cell* and *Inflorescence/culm-leaves indices* curves) and a low but constant presence of dicots phytoliths (cf. *D/P indices* curves), resembling an agroforestry system (Ferrara et al. 2023). Phase 3 at 70-60 cm is characterised by a higher peak of grasses reaching inflorescence (cf. *Inflorescence/culm-leaves index*), but associated with a slight decrease of dicots (cf. *D/P indices* curves) and long cells grasses (cf. *Long/short cell index*), transitioning into a further slight decrease of dicots (< 1%) (cf. *D/P indices*). The stratigraphy at 60 and 70 cm depth is characterised by the inclusion of highly fragmented small pottery samples, which could attest the anthropogenic use of the site at those layers. In the latest phase of the stratigraphic profile (Phase 4), we see the transition of this agroecosystem into a system characterised by an increase in the presence of dicots until today. Such increase may attest a historical transition in local land use practices from spatial arrangements typical of Class 1, where century-old olive trees were maintained at wide distances to provide space for other crops and/or grazing (as suggested by the phytolith record in Phase 3), to the spatial arrangement of Class 2, characterised by an intensification in the presence of olive trees, intermixed with new tree species.

## 5. Discussion

The results of our overlap analysis in terms of degrees of overlaps shown in Table 2 are an indication of the semantic relationships (cf. Ahlqvist 2008) between the land use classes mapped in the image.

In the case of the overlap between Class/Conceptual space 1 (Orchard of century-old olive trees) and Class/Conceptual space 2 (Mediterranean garden), the diverse percentages of overlap show that a Mediterranean garden (Class 2) is more similar to an orchard of

century-old olive trees (Class 1) than vice versa (76.6% vs 7.5%). Spatially, 76.6% of the mapped Mediterranean gardens (Class 2) are located in the 7.5% mapped Orchards of century-old olive trees (Class 1) (Figure 8). These figures signify that locals have turned 7.5% of their old olive orchards into Mediterranean gardens by planting new and different trees (e.g. almond, citrus, fruit trees) among old olives, which now constitutes 76.6% of the entire surface mapped in the image as Mediterranean gardens. Such a high percentage (76.6%) is furthermore informative as it provides insights into local past practices of land use. The presence of olive trees may have been considered fundamental for the good design and spatial arrangement of a Mediterranean garden, a practice already encountered in intercropping agroecosystems in Antiquity (cf. Ferrara et al. 2023). From the overlap analysis between these two classes of the same land use, we can therefore understand that, when locals decided to arrange a certain area as a Mediterranean garden, they planted the garden trees around and/or in between already existing old olive trees (cf. Figure 12 and Figure 13 for further visual clarification).

The results from our overlap analysis allows for further queries as, for instance, about the semantic relationships between the diverse conceptualisations of the use of space that these two classes represent, at different temporalities. The idea to arrange a place as a Mediterranean garden could have been responded to new and different logics in the use of space, not conceptualised anymore as an orchard with olives as the main crop. Nevertheless, their overlap to a certain degree shows how they contain spatio-temporal elements also present in previous conceptual spaces of the same land use (i.e. the olive trees are still kept as an important component in the new gardens). Furthermore, while these land use shifts are temporally linear, they may have not been unidirectional (only from orchards to gardens). Potentially, there could have been oscillation dynamics in time between these two conceptual spaces, with fruit tree plantations (Conceptual space 2) in between century-old olive trees (Conceptual space 1) at diverse periods in time (cf. results of change analysis done in Ferrara et al. 2024b, attesting the past presence in the study area of fruit tree varieties, nowadays disappeared). As such, also gardens, likewise century-old olive trees, could have thus acted as spatial filter (Wästfelt 2021), influencing the next spatial configurations of local land use. It is in these oscillations between different conceptual spaces of land use that biocultural heritage of historical landscapes is formed at different points in time and preserved until the present, and the method from Ferrara et al. 2024a implemented here is able to map it.

In the case of the overlap between Class 1 and Class 3, the percentages obtained from our analysis indicate that 26.6% of all the intensive plantations mapped in the image (Class 3) have been placed in between century-old olive trees (Class 1) (7.9% of the entire surface mapped as such). From an agricultural perspective, such a land use pattern is reasonable since intensive monoplantations are usually spatially arranged in a geometric fashion, where the presence of randomly scattered century-old olive trees represents an impediment for mechanical tilling and harvest. Moreover, intensive plantations are usually located on plain grounds, while century-old olive trees are spread on slopes. These considerations can explain the low percentage of overlap between these two classes in the study area.

The methodological approach presented in this paper shows that, by analysing remnants of old vegetation in current landscapes, we can understand how certain elements of past agroecosystems have or have not been taken into account in the design of new plantations. This is evident, for instance, in the passage from orchards of century-old olive trees to respectively fruit gardens or to intense olive plantations, the former an example of maintenance, the latter of radical change. Moreover, the fact that only 7.5% of century-old



**Figure 12.** (a) Example of an area in the input image where the Class 1 (Orchards of century-old olive trees) and Class 2 (Mediterranean gardens) partially overlap; (b) the arrows indicate the location of some new fruit trees that locals have planted among the century-old olive trees (Class 1) within the framework of conceptual space and Class 2 (Mediterranean garden). It is the presence of these fruit trees among century-old olive trees that allows the same space to be classified as both Class 1 (Orchards of century-old olive trees) and Class 2 (Mediterranean gardens).

olive trees orchards have been transformed into 76.6% of Mediterranean gardens tells us that the 92.5% of century-old olive orchards have remained the same until today, still a representation of a deep land use history. As such, the different degrees of overlap between the geospatial classes extracted provide direct information to understand and characterise better the nature of these land use changes. At the same time, the high percentage of Mediterranean gardens created on ancient olive trees' surfaces may indicate that the presence of century-old olive trees was considered an important ecological component in this system (due to its presence at 76.57%) and, for such reason, they have always been kept alive, while intercropped with other trees. Overall, these transitions dynamics represent a crucial aspect of historical agricultural landscapes that the geospatial method presented in this paper is able to map by analysing local land use spatial patterns from a single orthoimage.

Together with standard remote sensing validation procedures, the major transition patterns traceable with our geospatial technique are validated also by reconstructions of land use dynamics spanning over millennia based on other proxies (plant microfossils). This is



**Figure 13.** Ground view of Conceptual space 2, Mediterranean garden (note the old olive tree on the left, intercropped with citrus trees and opuntia).

demonstrated by phytolith analysis from Profile A, which tells the story of the progressive transition from a typical shrubland, first crafted into an agroforestry system spatially represented by what we have defined as Conceptual space 1, turned today into a more and more open environment. Similarly, the historical passage from agroforestry (Conceptual space 1) to fruit intercropping spatial model of land arrangement (Conceptual space 2) and the potential oscillations in time between these two conceptual spaces of land use are traceable in the phytoliths signal of Profile B, since the presence of dicots phytoliths is constant along the profile. As such, we can argue that the supervised contextual post-classification technique we have applied in this paper allows for unpacking the spatial and temporal trajectories of land use in a given area, by detecting oscillations between diverse spatial configurations that both persist over time and change in their category semantic.

Normally whatever change analysis in remote sensing is framed within temporal perspectives covering relatively short and recent times, and by comparing a past and a later state of the same location, as depicted by two or more images (cf. Ferrara et al. 2024b). Land use processes with a deep history of human-nature interactions have spatio-temporal gradients of change (and persistence) which can only be approached by adopting a long-term historical perspective. Ahlqvist (2008) showed the possibility to categorise semantically heterogeneous land cover classes. Instead of seeing overlapping geospatial classes (the same pixels classified as belonging to more than one class at once) as evidence of category uncertainty, or as due to semantic incompatibility and classification errors (cf. Shi et al. 2004 consider overlay as error), the results from our overlap analysis demonstrate that different classes can be mutually inclusive and at different degrees. It is exactly such overlap that qualitatively expands the spatial analysis done, since it allows reaching valuable information related not only to the spatial dimension of the classes extracted, but to their temporal dimensions as well. In this analytical process, the use of a single Earth observation product does not represent a limitation of our methodological approach. On the contrary, it

represents a research advance that still needs to be adequately explored within the remote sensing community and a complementary method to more standard change analyses.

## 6. Conclusions

In this paper, by computationally extracting and mapping physical representations of diverse temporalities of the same land use from just one digital image, we have demonstrated that it is possible to understand and represent the dynamicity of the landscape as land use phenomena occurring and overlapping each other over time. This possibility relies on the presence of biocultural traces constantly left by land use practices on a landscape along history and their use as geospatial representations of present-past dynamics. As such, our work shows how just a single Earth observation product contains multidimensional information that can be extracted and explored in their changing semantics, and this information can be employed for qualitative studies even within a long-term perspective, especially when combined with archaeological landscape surveys and botanical proxy data as cross-validation.

When generalised to historical land use and landscape research, our methodological approach demonstrates that contextual geospatial analysis on remote sensing products can identify not only ongoing land use but also their temporal connections with previous land uses (Ahlqvist et al. 2012). The spatial structure and distribution of past legacies in current landscapes can be used to gain a historical understanding of past land use functions and practices. This knowledge helps us reconstruct and thus access how agroecosystems and landscapes have evolved and responded to anthropogenic use. Similar analysis can be done in other geographical contexts having different social, cultural and ecological histories than the case study presented in this paper. Further research is necessary, to test the potentialities of our methodological approach in other contexts, using different types of input images and training areas, developing and testing new validation approaches and datasets (e.g. other environmental and/or historical proxies rather than only archaeobotanical evidence).

In conclusion, we argue that our work demonstrates the potentiality of contextual geospatial analysis to advance the knowledge about human-nature dynamics crossing different time scales, *within the same space*. This may help understand better the ecological and socio-cultural evolution of specific landscape processes along time, such as the role that the maintenance of certain agricultural practices (as the olive cultivation) has played for the preservation of local agrobiodiversity and soil health, as well as for the adaptation to climate change. All research findings having practical implications for contemporary and future sustainable management of these historical landscapes.

## Notes

1. [https://docs.qgis.org/3.34/en/docs/user\\_manual/processing\\_algs/qgis/vectoranalysis.html#qgiscalculatevectoroverlaps](https://docs.qgis.org/3.34/en/docs/user_manual/processing_algs/qgis/vectoranalysis.html#qgiscalculatevectoroverlaps) (Last accessed 15 January 2025).
2. <https://www.phytcare.org>.

## Acknowledgements

We would like to thank Michael Lindblom, Martin Finné and Anneli Ekblom for key insights on the earlier version of the article, Pascoal Gota for assistance in running the age-depth model and Johan Lindberg for support on statistical analysis. Our deepest gratitude goes also to the anonymous reviewers for the precious comments that helped improve significantly the breath and quality of our manuscript.



## Ethical approval

No ethical considerations were required.

## Disclosure statement

No potential conflict of interest was reported by the author(s).

## Research data

The geospatial data underlying this study are available as [supplementary material](#) of the paper Ferrara et al. 2024a.

Data on phytolith analysis used for cross-validation are available as [supplementary material](#) at the following link on Figshare: <https://doi.org/10.6084/m9.figshare.27063505.v1>

## Funding

This work was supported by the Swedish Research Institute – Vetenskapsrådet research project ‘Oliven och Siciliens bio-kulturella arv’, grant number 2020-02625. The orthophoto used for the analysis has been granted by *Regione Siciliana, Assessorato Regionale Territorio e Ambiente, Dipartimento di Urbanistica, Area 2 Interdipartimentale*, on 31/01/2023 with authorisation number n. 2023-S-3466.

## References

- [dataset] European Environmental Agency (EEA). 2020. CORINE Land Cover 2018 (vector), Europe, 6-yearly - version 2020\_20u1. [accessed 2025 Jan 15]. <https://sdi.eea.europa.eu/catalogue/copernicus/api/records/71c95a07-e296-44fc-b22b-415f42acdf0?language=all>.
- Ahlqvist O, Wästfelt A, Nielsen M. 2012. Formalized interpretation of compound land use objects – mapping historical summer farms from a single satellite image. *J Land Use Sci.* 7(1):89–107. doi: [10.1080/1747423X.2010.537787](https://doi.org/10.1080/1747423X.2010.537787).
- Ahlqvist O. 2005. Using uncertain conceptual spaces to translate between land cover categories. *Int J Geogr Inf Sci.* 19(7):831–857. doi: [10.1080/13658810500106729](https://doi.org/10.1080/13658810500106729).
- Ahlqvist O. 2008. Extending post classification change detection using semantic similarity metrics to overcome class heterogeneity: a study of 1992 and 2001 national land cover database changes. *Remote Sens Environ.* 112(3):1226–1241. doi: [10.1016/j.rse.2007.08.012](https://doi.org/10.1016/j.rse.2007.08.012).
- Aleman JC, Canal-Subitani S, Favier C, Bremond L. 2014. Influence of the local environment on lacustrine sedimentary phytolith records. *Palaeogeogr Palaeoclimatol Palaeoecol.* 414:273–283. doi: [10.1016/j.palaeo.2014.08.030](https://doi.org/10.1016/j.palaeo.2014.08.030).
- Alexandre A, Meunier J-D, Lézine A-M, Vincens A, Schwartz D. 1997. Phytoliths: indicators of grassland dynamics during the late Holocene in intertropical Africa. *Palaeogeography, Palaeoclimatology, Palaeoecology.* 136(1-4):213–229. doi: [10.1016/S0031-0182\(97\)00089-8](https://doi.org/10.1016/S0031-0182(97)00089-8).
- Alias B, Karthika R, Parameswaran L. 2018. Classification of High Resolution Remote Sensing Images using Deep Learning Techniques. *International Conference on Advances in Computing, Communications and Informatics (ICACCI)*, p. 1196–1202.
- Anderson JR, Hardy EE, Roach JT, Witmer RE. 1976. A land use and land cover classification system for use with remote sensor data. Washington (DC): U.S. Government Publishing Office.
- Arnan X, López BC, Martínez-Vilalta J, Estorach M, Poyatos R. 2012. The age of monumental olive trees (*Olea europaea*) in northeastern Spain. *Dendrochronologia.* 30(1):11–14. doi: [10.1016/j.dendro.2011.02.002](https://doi.org/10.1016/j.dendro.2011.02.002).
- Barthel S, Crumley CL, Svedin U. 2013. Bio-cultural refugia—safeguarding diversity of practices for food security and biodiversity. *Global Environ Change.* 23(5):1142–1152. doi: [10.1016/j.gloenvcha.2013.05.001](https://doi.org/10.1016/j.gloenvcha.2013.05.001).
- Belcore E, Piras M, Wozniak E. 2020. Specific alpine environment land cover classification methodology: google Earth Engine processing for Sentinel-2 data. *Int Arch Photogramm Remote Sens Spatial Inf Sci.* XLIII-B3-2020:663–670. doi: [10.5194/isprs-archives-XLIII-B3-2020-663-2020](https://doi.org/10.5194/isprs-archives-XLIII-B3-2020-663-2020).

- Bernabei M. 2015. The age of the olive trees in the Garden of Gethsemane. *J Archaeol Sci.* 53:43–48. doi: [10.1016/j.jas.2014.10.011](https://doi.org/10.1016/j.jas.2014.10.011).
- Blaauw M, Christen J, Aquino Lopez M. 2022. rbacon: age-depth modelling using Bayesian statistics. R Package Version 2.5.8.
- Bremont L, Alexandre A, Peyron O, Guiot J. 2005. Grass water stress estimated from phytoliths in West Africa. *J Biogeogr.* 32(2):311–327. doi: [10.1111/j.1365-2699.2004.01162.x](https://doi.org/10.1111/j.1365-2699.2004.01162.x).
- Bremont L, Alexandre A, Wooller MJ, Hély C, Williamson D, Schäfer PA, Majule A, Guiot J. 2008. Phytolith indices as proxies of grass subfamilies on East African tropical mountains. *Global Planet Change.* 61(3-4):209–224. doi: [10.1016/j.gloplacha.2007.08.016](https://doi.org/10.1016/j.gloplacha.2007.08.016).
- Butzer KW. 1980. Context in archaeology: an alternative perspective. *J Field Archaeol.* 7(4):417–422. doi: [10.2307/529520](https://doi.org/10.2307/529520).
- Camarero JJ, Colangelo M, Gracia-Balaga A, Ortega-Martínez M, Büntgen U. 2021. Demystifying the age of old olive trees. *Dendrochronologia.* 65:125802. doi: [10.1016/j.dendro.2020.125802](https://doi.org/10.1016/j.dendro.2020.125802).
- Camarero JJ, Touchan R, Valeriano C, Bashour I, Stephan J. 2024. Dating the Noah trees to improve age estimates in centennial and millennial olive trees. *Dendrochronologia.* 84:126181. doi: [10.1016/j.dendro.2024.126181](https://doi.org/10.1016/j.dendro.2024.126181).
- Cevasco R, Moreno D, Hearn R. 2015. Biodiversification as an historical process: an appeal for the application of historical ecology to bio-cultural diversity research. *Biodivers Conserv.* 24(13):3167–3183. doi: [10.1007/s10531-015-0943-3](https://doi.org/10.1007/s10531-015-0943-3).
- Cherubini P, Humbel T, Beeckman H, Gärtner H, Mannes D, Pearson C, Schoch W, Tognetti R, Lev-Yadun S. 2013. Olive tree-ring problematic dating: a comparative analysis on Santorini (Greece). *PLoS One.* 8(1):e54730. doi: [10.1371/journal.pone.0054730](https://doi.org/10.1371/journal.pone.0054730).
- Cohen M, Godron M, Cretin-Pablo R, Pujos R. 2023. Plant biodiversity in Mediterranean orchards is related to historical land use: perspectives for biodiversityfriendly olive production. *Reg Environ Change.* 23(2):70. doi: [10.1007/s10113-023-02067-6](https://doi.org/10.1007/s10113-023-02067-6).
- Couclelis H. 2009. The abduction of Geographic Information Science: transporting spatial reasoning to the realm of purpose and design. In: Hornsby KS, Claramunt C, Denis M, and G. Ligozat, editors. *Spatial information theory. COSIT 2009. Lecture notes in computer science*, Vol. 5756. Berlin, Heidelberg, Springer. p. 342–356.
- Crews-Meyer KA, Hudson PF, Colditz RR. 2004. Landscape complexity and remote classification in Eastern Coastal Mexico: applications of Landsat-7 ETM+ Data. *Geocarto Int.* 19(1):45–56. doi: [10.1080/10106040408542298](https://doi.org/10.1080/10106040408542298).
- Crumley CL. 1979. Three locational models: an epistemological assessment for anthropology and archaeology. In: Schiffer MB, editor. *Advances in archaeological method and theory*. Vol. 2. New York: Academic Press. p. 141–173.
- Crumley CL. 2000. From garden to globe: linking time and space with meaning and memory. In: McIntosh R, Tainter JA, McIntosh SK, editors. *The way the wind blows: climate, history, and human action*. Series in Historical Ecology. New York, Columbia University Press. p. 193–208.
- Crumley CL. 2019. New paths into the Anthropocene: applying historical ecologies to the human future (Part I, Chapter 1). In: Isendahl C, Stump D, editors. *The Oxford handbook of historical ecology and applied archaeology*. Oxford: Oxford University Press.
- de Bremond A. 2021. The emergence of land systems as the nexus for sustainability transformations. *Ambio.* 50(7):1299–1303. doi: [10.1007/s13280-021-01519-9](https://doi.org/10.1007/s13280-021-01519-9).
- Delhon C, Alexandre A, Berger JF, Thiébaud S, Brochier JL, Meunier JD. 2003. Phytolith assemblages as a promising tool for reconstructing Mediterranean Holocene vegetation. *Quat Res.* 59(1):48–60. doi: [10.1016/S0033-5894\(02\)00013-3](https://doi.org/10.1016/S0033-5894(02)00013-3).
- Delhon C, Binder D, Verdin P, Mazuy A. 2020. Phytoliths as a seasonality indicator? The example of the Neolithic site of Pendimoun, south-eastern France. *Veget Hist Archaeobot.* 29(2):229–240. doi: [10.1007/s00334-019-00739-0](https://doi.org/10.1007/s00334-019-00739-0).
- Delhon C, Martin L, Thiébaud S. 2024. Neolithic shepherds and sheepfold caves in Southern France and adjacent areas: an overview from 40 years of bioarchaeological analyses. *Quat Int.* 683-684:61–75. doi: [10.1016/j.quaint.2023.03.004](https://doi.org/10.1016/j.quaint.2023.03.004).
- Dixon DP, Jones JP. 1998. My dinner with derrida, or spatial analysis and poststructuralism do lunch. *Environ Plan A.* 30(2):247–260. doi: [10.1068/a300247](https://doi.org/10.1068/a300247).
- Feng Y, Jie D, Guo M, Dong S, Chen X, Liu H, Liu L, Li N. 2017. Phytolith loss and enrichment in soil phytolith assemblages revealed by comparisons of phytoliths in vegetation and surface soils of altitudinal belts in the Changbai Mountains, Northeast China. *Flora.* 236-237:84–93. doi: [10.1016/j.flora.2017.08.005](https://doi.org/10.1016/j.flora.2017.08.005).

- Ferrara V, Ekblom A, Wästfelt A. 2019. Biocultural heritage in Sicilian olive groves; the importance of heterogeneous landscapes over the long term. In: Goldstein IM and DellaSala DA, editors. 2020, *Encyclopedia of the world's biomes*. Amsterdam: Elsevier. p. 135–145.
- Ferrara V, Lindberg J, Wästfelt A. 2024a. CONTEXTS.py (CS.py): a supervised contextual post-classification method to access multiple dimensions of complex geospatial objects. *MethodsX*. 12:102753. doi: [10.1016/j.mex.2024.102753](https://doi.org/10.1016/j.mex.2024.102753).
- Ferrara V, Sala G, Ingemark D, La Mantia T. 2023. The “green” granary of the Empire? Insights into olive agroforestry in Sicily from the Roman past and the present. *Italian J Agron*. 18(1):2184. doi: [10.4081/ija.2023.2184](https://doi.org/10.4081/ija.2023.2184).
- Ferrara V, Sala G, La Mantia T. 2024b. Change and persistence in an olive landscape of Sicily. *Geospatial insights into biocultural heritage*. *Hum Ecol*. 52(2):353–366. doi: [10.1007/s10745-024-00498-1](https://doi.org/10.1007/s10745-024-00498-1).
- Ferrara V, Wästfelt A, Ekblom A. 2022. From landscape as heritage to biocultural heritage in a landscape. The ecological and cultural legacy of millennial land use practices for future natures. In Pettenati G, editor. *Landscape as heritage: critical perspectives*. London: Routledge. p. 80–90.
- Ferrara V, Wästfelt A. 2021. Unpacking layers of space-time complexity in land use dynamics. A case study from the olive agrosystems of Sicily (Italy). *giformum*. 1(2):108–121. doi: [10.1553/giscience2021\\_02\\_s108](https://doi.org/10.1553/giscience2021_02_s108).
- Ferrara V. 2016. Olive trees of sicily. A historical ecology [master thesis dissertation]. Uppsala: Department of Archaeology and Ancient History, Uppsala University.
- Ferrara V. 2024. Historical olive agroecosystems of sicily. In: Operationalising biocultural heritage for sustainable futures. *Studies in global archaeology*. Vo.l. 29. Uppsala: Acta Universitatis Upsaliensis. ISBN 978-91-506-3072-5.
- Foody GM. 2008. Harshness in image classification accuracy assessment. *Int J Remote Sens*. 29(11):3137–3158. doi: [10.1080/01431160701442120](https://doi.org/10.1080/01431160701442120).
- Gao Y, Li Q. 2019. A segmented particle swarm optimization convolutional neural network for land cover and land use classification of remote sensing images. *Remote Sens Lett*. 10(12):1182–1191. doi: [10.1080/2150704X.2019.1671633](https://doi.org/10.1080/2150704X.2019.1671633).
- Gärdenfors P. 2000. *Conceptual spaces: the geometry of thought*. Cambridge (MA): MIT Press.
- Gillson L, Dirk C, Gell P. 2021. Using long-term data to inform a decision pathway for restoration of ecosystem resilience. *Anthropocene*. 36:100315. doi: [10.1016/j.ancene.2021.100315](https://doi.org/10.1016/j.ancene.2021.100315).
- Gromny E, Lewiński S, Rybicki M, Malinowski R, Krupiński M, Nowakowski A, Jenerowicz M. 2019. Creation of training dataset for Sentinel-2 land cover classification. Poland: SPIE, Wilga. p. 106.
- Gurney MC, Townshend JRG. 1983. The use of contextual information in the classification of remote sensed data. *Photogramm Eng Remote Sens*. 49(1):55–64.
- Hägerstrand T. 1991. The landscape as overlapping neighbourhoods. In Carlestam G, Sollbe B, editor. *Om tidens vidd och tingens ordning*. Texter av Torsten Hägerstrand. Stockholm: Byggnadsforskingsrådet. p. 47–55.
- Hodder I, Hutson S. 2003. Contextual archaeology. In: Hodder I, Hutson S, editors. *Reading the past: current approaches to interpretation in archaeology*. Cambridge: Cambridge University Press. p. 156–205.
- Hodder I. 1985. New generations of spatial analysis in archaeology. In: Burillo F, editor. *Arqueologia Espacial*. Teruel: Colegio Universitario Teruel.
- Howarth JT. 2008. *Landscape and purpose: modeling the functional and spatial organization of the land* [Ph.D. thesis]. Santa Barbara, CA: University of California.
- Mader A, Langer M, Knippers J, Speck O. 2020. Learning from plant movements triggered by bulliform cells: the biomimetic cellular actuator. *J R Soc Interface*. 17(169):20200358. doi: [10.1098/rsif.2020.0358](https://doi.org/10.1098/rsif.2020.0358).
- Massey D. 1999. Space-time, ‘Science’ and the relationship between physical geography and human geography. *Trans Inst British Geogr*. 24(3):261–276. doi: [10.1111/j.0020-2754.1999.00261.x](https://doi.org/10.1111/j.0020-2754.1999.00261.x).
- Mazuy A, Ferrara V, Ekblom A, Delhon C. 2024. A rapid and simple method for the extraction of biogenic silica (BSi) in phytolith-poor sediments and soils. *MethodsX*. 12:102634. doi: [10.1016/j.mex.2024.102634](https://doi.org/10.1016/j.mex.2024.102634).
- Mehmood M, Shahzad A, Zafar B, Shabbir A, Ali N. 2022. Remote sensing image classification: a comprehensive review and applications. *Math Prob Eng*. 2022:1–24. doi: [10.1155/2022/5880959](https://doi.org/10.1155/2022/5880959).
- Neumann K, Strömberg CAE, Ball T, Albert RM, Vrydaghs L, Scott Cummings L. 2019. International code for phytolith nomenclature (ICPN) 2.0. *Ann Bot*. 124(2):189–199. doi: [10.1093/aob/mcz064](https://doi.org/10.1093/aob/mcz064).
- Nielsen MM, Heurich M, Malmberg B, Brun A. 2014. Automatic mapping of standing dead trees after an insect outbreak using the Window Independent Context Segmentation method. *J For*. 112(6): 564–571.

- Nielsen MM. 2015. Remote sensing for urban planning and management: the use of window-independent context segmentation to extract urban features in Stockholm. *Comput Environ Urban Syst.* 52:1–9. doi: [10.1016/j.compenvurbsys.2015.02.002](https://doi.org/10.1016/j.compenvurbsys.2015.02.002).
- Padilla R, Netto SL, da Silva EAB. 2020. A survey on performance metrics for object-detection algorithms. *International Conference on Systems, Signals and Image Processing (IWSSIP)*, 237–242 (2000).
- Pan X, Wang Z, Gao Y, Dang X, Han Y. 2022. Detailed and automated classification of land use/land cover using machine learning algorithms in Google Earth Engine. *Geocarto Int.* 37(18):5415–5432. doi: [10.1080/10106049.2021.1917005](https://doi.org/10.1080/10106049.2021.1917005).
- Pearsall DM, Trimble MK. 1984. Identifying past agricultural activity through soil phytoliths analysis: a case study from the Hawaiian Islands. *J Archaeol Sci.* 11(2):119–133. doi: [10.1016/0305-4403\(84\)90047-5](https://doi.org/10.1016/0305-4403(84)90047-5).
- Pearsall DM. 2015. *Paleoethnobotany. A handbook of procedures.* New York: Routledge.
- Piperno DR. 1988. *Phytolith analysis: an archaeological and geological perspective.* San Diego: Academic Press.
- R Core Team. 2021. *R: a language and environment for statistical computing.* Vienna: R Foundation for Statistical Computing.
- Reimer P, Austin WEN, Bard E, Bayliss A, Blackwell PG, Ramsey CB, Butzin M, Cheng H, Edwards RL, Friedrich M, et al. 2020. The IntCal20 Northern Hemisphere radiocarbon age calibration curve 0–55 cal kbp. *Radiocarbon.* 62(4):725–757. doi: [10.1017/RDC.2020.41](https://doi.org/10.1017/RDC.2020.41).
- Rencheng L, Fan J, Carter J, Jiang N, Gu Y. 2017. Monthly variation of phytoliths in the leaves of the bamboo *Dendrocalamus ronganensis* (Poaceae: bambusoideae). *Rev Palaeobot Palynol.* 246:62–69. doi: [10.1016/j.revpalbo.2017.06.006](https://doi.org/10.1016/j.revpalbo.2017.06.006).
- Sangster AG. 1970. Intracellular silica deposition in immature leaves in three species of the Gramineae. *Annals of Botany.* 34(1):245–257. doi: [10.1093/oxfordjournals.aob.a084359](https://doi.org/10.1093/oxfordjournals.aob.a084359).
- Schicchi R, Raimondo MF. 2011. Schede per il censimento degli alberi monumentali di Sicilia 37–43. Palermo: Quaderni di Botanica Ambientale e Applicata - PLANTA, 22, p. 135–150.
- Shabbir A, Rasheed A, Shehraz H, Saleem A, Zafar B, Sajid M, Ali N, Dar SH, Shehryar T. 2021. Detection of glaucoma using retinal fundus images: A comprehensive review. *Math Biosci Eng.* 18(3): 2033–2076. doi: [10.3934/mbe.2021106](https://doi.org/10.3934/mbe.2021106).
- Shi C, Zhang X, Sun J, Wang L. 2022. Remote sensing scene image classification based on self-compensating convolution neural network. *Remote Sens.* 14(3):545. doi: [10.3390/rs14030545](https://doi.org/10.3390/rs14030545).
- Shi W, Cheung CK, Tong X. 2004. Modelling error propagation in vector-based overlay analysis. *Isprs – J Photogramm Remote Sens.* 59(1-2):47–59. doi: [10.1016/j.isprsjprs.2004.05.003](https://doi.org/10.1016/j.isprsjprs.2004.05.003).
- Soubry I, Robinov L, Chu T, Guo X. 2022. Mapping shrub cover in grasslands with an object-based approach and investigating the connection to topo-edaphic factors. *Geocarto Int.* 37(27):16926–16950. doi: [10.1080/10106049.2022.2120549](https://doi.org/10.1080/10106049.2022.2120549).
- Strömberg CAE, Dunn RE, Crifò C, Harris EB. 2018. Phytoliths in paleoecology: analytical considerations, current use, and future directions. In: Croft DA, Su DF and Simpson SW, editors. *Methods in paleoecology.* Cham: Springer. p. 235–287.
- Strömberg CAE, Werdelin L, Friis EM, Saraç G. 2007. The spread of grass-dominated habitats in Turkey and surrounding areas during the Cenozoic: phytolith evidence. *Palaeogeogr Palaeoclimatol Palaeoecol.* 250(1-4):18–49. doi: [10.1016/j.palaeo.2007.02.012](https://doi.org/10.1016/j.palaeo.2007.02.012).
- Thomas IL, Allcock, GM. 1984. Determining the confidence level for a classification. *Photogramm Eng Remote Sens.* 50(10):1491–1496.
- Urwin N. 2013. Spatial distribution of old olive trees. In: Given M, Bernard Knapp A, Noller J, Sollars L and Kassianidou V, editors. *Landscape and interaction. The troodos archaeological and environmental survey project, cyprus.* Oxford: Oxbow Books, Vol. I, p. 311–314.
- Van Genderen JL, Lock BE, Vass PA. 1978. Remote Sensing: statistical testing of thematic map accuracy. *Remote Sens Environ.* 7(1):3–14. doi: [10.1016/0034-4257\(78\)90003-2](https://doi.org/10.1016/0034-4257(78)90003-2).
- Wästfelt A, Arnberg W. 2013. Local spatial context measurements used to explore the relationship between land cover and land use functions. *Int J Appl Earth Obs Geoinf.* 23:234–244. doi: [10.1016/j.jag.2012.09.006](https://doi.org/10.1016/j.jag.2012.09.006).
- Wästfelt A. 2009. Land use qualities identified in remotely-sensed images. *Int J Remote Sens.* 30(9): 2411–2427. doi: [10.1080/01431160802552694](https://doi.org/10.1080/01431160802552694).
- Wästfelt A. 2015. Reclaiming position: using local context to visualise interpretations of satellite images in humanities and social science. *J Art History.* 84(2):108–122. doi: [10.1080/00233609.2015.1031696](https://doi.org/10.1080/00233609.2015.1031696).
- Wästfelt A. 2021. Landscape as filter - farm adaptation to changing contexts. *J Land Use Sci.* 16(2):142–158. doi: [10.1080/1747423X.2021.1879296](https://doi.org/10.1080/1747423X.2021.1879296).

- Yang Z, Jiang W, Lin Y, Elberink SO. 2020. Using training samples retrieved from a topographic map and unsupervised segmentation for the classification of airborne laser scanning data. *Remote Sensing*. 12(5):877. doi: [10.3390/rs12050877](https://doi.org/10.3390/rs12050877).
- Zapata-Pérez J, Doménech-Asensi G, Ruiz-Merino R, Martínez-Álvarez JJ, Fernández-Berni J, Carmona-Galán R. 2020. Fixed pattern noise analysis for feature descriptors in CMOS APS images. *Sens Imaging*. 21(1), 1–24. doi: [10.1007/s11220-020-0278-3](https://doi.org/10.1007/s11220-020-0278-3).